Development of a novel model to estimate bedding factors to ensure the economic and robust design of rigid pipes under soil loads

Alzabeebee, Saif; Chapman, David; Faramarzi, Asaad

DOI:
10.1016/j.tust.2017.11.009

Document Version
Peer reviewed version

Citation for published version (Harvard):
Alzabeebee, S, Chapman, D & Faramarzi, A 2017, 'Development of a novel model to estimate bedding factors to ensure the economic and robust design of rigid pipes under soil loads', *Tunnelling and Underground Space Technology*. https://doi.org/10.1016/j.tust.2017.11.009

Development of a novel model to estimate bedding factors to ensure the economic and robust design of rigid pipes under soil loads

Saif Alzabeebee (Corresponding author)

Department of Civil Engineering, School of Engineering, University of Birmingham, Birmingham, B15 2TT, UK

Department of Civil Engineering, College of Engineering, University of Al-Qadisiyah, Al-Qadisiyah, Iraq

E-mail: Saif.Alzabeebee@gmail.com

David N Chapman

Department of Civil Engineering, School of Engineering, University of Birmingham, Birmingham, B15 2TT, UK

E-mail: D.N.Chapman@bham.ac.uk

Asaad Faramarzi

Department of Civil Engineering, School of Engineering, University of Birmingham, Birmingham, B15 2TT, UK

E-mail: A.Faramarzi@bham.ac.uk

Abstract

Buried concrete pipes are load bearing structures that need to resist the loads imposed by the surrounding ground. The common approach to design buried concrete pipes is based on an empirical method called the Indirect Design Method, which uses the laboratory capacity of the buried pipe linked to the field capacity using an empirical factor known as the bedding factor. However, limited published studies have investigated this bedding factor or tried to improve the current bedding factor values. Therefore, this study investigated the bending moment and bedding factor for concrete pipes under soil loads by conducting a parametric study investigating the effect of the installation condition, pipe diameter, pipe thickness and backfill height. A validated finite element model has been used for this purpose. The bedding factors obtained from the analyses have been compared with the bedding factors currently adopted by the AASHTO and British Standard (BS) design standards. The results showed that the BS design standard is conservative. In addition, the AASHTO design standard has been shown not to be safe for pipes with a diameter of 0.3 m and becomes more conservative as the diameter increases or the installation quality decreases. Therefore, new bedding factor models have been proposed using the results of the finite element modelling utilising an evolutionary polynomial regression (EPR) method. The paper demonstrates that the new models could be used for the economic and robust design of concrete pipes. The proposed models in this paper have the potential to significantly reduce the costs involved in either construction or maintenance of buried concrete pipes.

Keywords: Concrete Pipes; Indirect Design Method; Bedding Factor; AASHTO; British Standards; Evolutionary Polynomial Regression.

Nomenclature

DP (kN/m)	the laboratory capacity of the pipe
BF	the bedding factor
W_t (kN/m)	the total force applied on the pipe in the field
SW95	well-graded sand with a degree of compaction of 95% of the Standard Proctor test
SW90	well-graded sand with a degree of compaction of 90% of the Standard Proctor test
SW85	well-graded sand with a degree of compaction of 85% of the Standard Proctor test
ML95	sandy silt with a degree of compaction of 95% of the Standard Proctor test
ML90	sandy silt with a degree of compaction of 90% of the Standard Proctor test
GP90	poorly graded gravelly sand with a degree of compaction of 90% of the Standard Proctor test
f_c' (kPa)	the compressive strength of the concrete
E_c (kPa)	the modulus of elasticity of the concrete
υ	Poisson ratio
γ (kN/m^3)	unit weight of the soil
c'(kPa)	cohesion of the soil
ϕ'(°)	angle of internal friction of the soil
K	Modulus number
R_f	Failure ratio
n	Modulus exponent
r (m)	the radius of the pipe measured to the centre of the pipe wall
VAF	is the vertical arching factor
H (m)	the backfill height
D_{out} (m)	the outside diameter of the pipe
D (m)	The inside diameter of the pipe
t (m)	the wall thickness of the pipe
CD	the coefficient of determination

1. Introduction

Buried rigid pipes are usually designed using the Indirect Design Method, which uses the field capacity of the buried pipe linked to the laboratory capacity (i.e. the pipe is tested without soil surround) using an empirical factor called the bedding factor (BF) as shown in Equation 1 (AASHTO, 2016; BSI, 2010). The laboratory test is called the three-edge bearing test, which involves the pipe being supported at the invert only and loaded by a line load at the pipe crown (further details on the test can be found in Moser and Folkman, 2008). The force which causes a crack of 0.254 mm is considered as the laboratory capacity of the pipe (MacDougall et al., 2016).

$$DP = \frac{Field\ capacity}{BF} \quad (1)$$

$$Field\ capacity = W_t \times FS \quad (2)$$

Where, DP is the laboratory capacity of the pipe, BF is the bedding factor, W_t is the total force applied on the pipe in the field and FS is the factor of safety. The total force is calculated by multiplying the overburden pressure above the crown of the pipe by an appropriate vertical arching factor. The value of the vertical arching factor depends on the burial condition (AASHTO, 2016; BSI, 2010).

As part of the present study, a review has been conducted of the British Standard (BS) (BSI, 2010) and the America Association of State Highway and Transportation Officials (AASHTO) standard (AASHTO, 2016). The review showed that the bedding factor values are significantly different between these two standards indicating considerable uncertainty in the methodology. In the BS, the bedding factor values range from 1.1 to 3.4 depending on the burial condition (BSI, 2010). However, in the AASHTO standard it ranges from 1.7 to 4.4 depending on the pipe diameter and

burial condition (AASHTO, 2016). Therefore, a thorough literature review has been conducted on the design and behaviour of concrete pipes to understand the reason of this discrepancy. Surprisingly, limited published studies have investigated bedding factors or tried to improve the current design bedding factors, with only two recent studies being found on bedding factors (MacDougall et al., 2016; Petersen et al., 2010). MacDougall et al., (2016) investigated the bedding factor for 0.6 m and 1.2 m inside diameter concrete pipes buried using the AASHTO Type 2 installation condition (i.e. the pipe is well supported in the haunch zone) under the AASHTO truck load and deep soil fill using experimental based studies. A large test pit was used for the pipe tests using an AASHTO truck load with depth of burial of 0.6 m and 1.2 m. In addition, test was also performed in a biaxial cell on the 0.6 m diameter pipe to simulate the case of a pipe buried in an embankment condition under deep burial fill. The pipe was tested by applying a maximum pressure of 700 kPa. MacDougall et al., (2016) found that the bedding factors recommended in AASHTO (2012) and AASHTO (2013) for soil load and traffic load are conservative, where the ratio of the recommended bedding factor to the obtained bedding factor ranged from 1.17 to 2.56. However, the MacDougall et al., (2016) study did not investigate the bedding factors for other AASHTO installation conditions (i.e. Type 1, Type 3 and Type 4), nor did it study the effect of the pipe diameter and pipe wall thickness on the bedding factor. Petersen et al., (2010) investigated the bedding factors of buried concrete pipes under the AASHTO truck live load using three-dimensional finite element modelling, where a single axle load was considered with a maximum tyre stress of 683 kPa multiplied by a dynamic impact factor. The bedding factors were derived under traffic load only by subtracting the bending moment due to backfill soil pressure. Therefore, the bedding factors obtained were only for live loads. The

conservatism of the AASHTO soil load bedding factors is due to the fact that these bedding factors were derived using the SPIDA finite element program (MacDougall et al., 2016). SPIDA adopts a Heger pressure distribution which, unfortunately, does not simulate the correct soil pressure distribution around the pipe (MacDougall, 2014) and leads to a very conservative design of buried concrete pipes (Allard and El Naggar, 2016). Hence, the AASHTO soil load bedding factors should be updated to enable more economical and robust designs of buried pipes.

In summary, based on this review, it can be concluded that the current AASHTO bedding factors are derived based on an inaccurate assumption of the soil pressure distribution. This inaccurate soil pressure distribution provides inaccurate designs, as demonstrated by MacDougall et al. (2016). In addition, the review showed that different values of bedding factor are considered in the ASSHTO standard and the BS, although the installation conditions are approximately similar. This indicates that there is considerable uncertainty in both design standards. Hence, it is necessary to do an extensive study based on a robust methodology to investigate the bedding factors and clarify the aforementioned issues. This could help future designs of buried pipes to be more economic and provide more confidence in the design methodologies. Therefore, the present study aimed to:

1- Develop a robust finite element model to predict the bending moment in the pipe wall under an applied soil load. Developing a valid model to predict the bending moment in the pipe wall is important in this study as the bending moment is used to calculate the bedding factor (Petersen et al., 2010; Young and O'Reilly, 1987).

2- Study the effect of installation condition, backfill height, pipe diameter and pipe wall thickness on the maximum bending moment in the pipe wall under soil loads.
3- Investigate the sensitivity of the soil load bedding factor to the parameters mentioned in point 2.
4- Develop surrogate models to predict the bedding factor and enable a robust and economical design of concrete pipes under different installation conditions.

2. Current practice to determine bedding factor values

The bedding factor depends on the installation condition of the buried pipe (AASHTO, 2016; BSI, 2010). In the AASHTO standard (AASHTO, 2016), there are four standard types of installation depending on the quality of the backfill. Type 1 is the highest quality where the pipe is fully supported in the haunch area while Type 4 is the poorest quality where the pipe is installed directly on the native soil with poor compaction provided in the haunch zone. Furthermore, the bedding factor value in the AASHTO standard depends on the diameter of the pipe. Figure 1 shows the condition of the haunch and bedding soils for each installation type. Table 1 shows the soil load bedding factor values currently adopted in the AASHTO standard (AASHTO, 2016).

The bedding factors used in the BS (BSI, 2010) also depend on the installation quality, but are independent on the diameter of the pipe. Currently, there are two general installation types. The first type is called concrete bedding, where the pipe is supported by reinforced or plain concrete in the bedding and haunch zone (Young and O'Reilly, 1987). The second type is called the granular bedding or natural base

(Young and O'Reilly, 1987). Each of these installation types are divided into classes depending on the quality of the pipe surround materials. Only the second type will be considered in this paper as it is more practical and is comparable to the AASHTO installation types. Table 2 shows the installation classes and the current bedding factor values for each class of granular bedding or natural base installation (BSI, 2010; Young and O'Reilly, 1987). It should be noted that the same terminology used in both the AASHTO standard (Type 1, 2, 3 and 4) and BS (class S, B, F, N and DD) were used to avoid confusion, and ensure designers easily understand the support condition of the pipe from the referred name without the need to go through the modelling details.

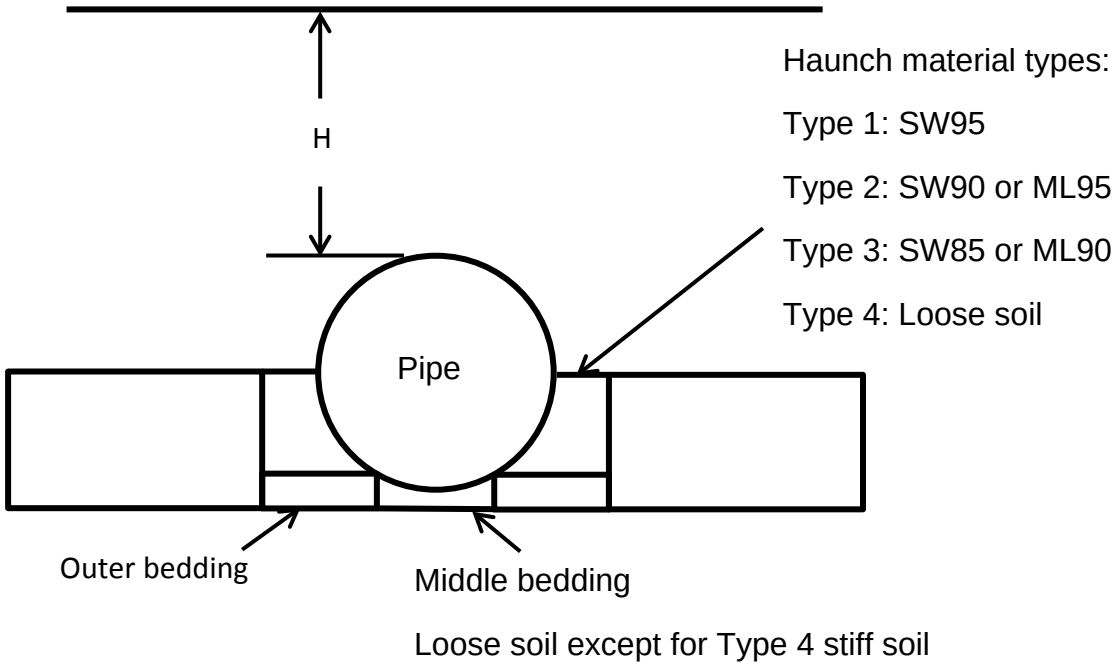

Figure 1: AASHTO installation types (AASHTO, 2016) (Note: SW is well-graded sand or gravelly sand; ML is sandy silt)

Table 1: Soil load bedding factors adopted in the current AASHTO standard (AASHTO, 2016)

Pipe diameter (m)	Standard installations			
	Type 1	Type 2	Type 3	Type 4
0.3	4.4	3.2	2.5	1.7
0.61	4.2	3.0	2.4	1.7
0.91	4.0	2.9	2.3	1.7
1.83	3.8	2.8	2.2	1.7
3.66	3.6	2.8	2.2	1.7

Table 2: Installation classes of granular bedding or natural base installation according to the British Standard (BSI, 2010; Young and O'Reilly, 1987)

Installation configuration	Installation class	Bedding factor
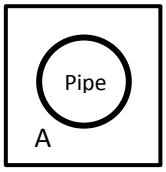	S	2.2
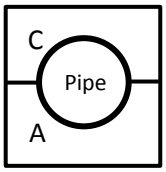	B	1.9 to 2.3
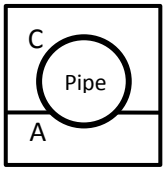	F	1.5 to 1.9
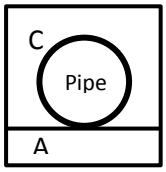	N	1.1 to 1.3
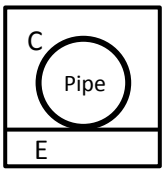	DD	1.1 to 1.3

(Note: A, single size granular material; C, backfill soil free of tree roots, frozen soil, clay lamps, stones larger than 40 mm or any material larger than 75 mm; E, natural soil)

3. Development of the finite element modelling

MacDougall (2014) reported the bending moments associated with a reinforced concrete pipe buried under different backfill heights (0.3 m, 0.6 m and 0.9 m) and loaded at the ground surface with an AASHTO tyre load of 100 kN with a tyre print area of 0.25 m x 0.5 m. The inner diameter of the pipe was 0.6 m with a wall thickness of 0.094 m. The compressive strength of the concrete (f_c') was 66000 kPa (9572.5 psi). The thickness of the bedding soil beneath the pipe was 95.5 cm to avoid the influence of the rigid boundary of the test pit base. This bedding soil was followed by a 7.5 cm layer of loose bedding soil to provide a uniform support for the pipe in the haunch zone. The surrounding and backfill soils were poorly graded sandy gravel with a minimum degree of compaction of 90 % of the Standard Proctor dry density.

As part of the present study, MIDAS GTS/NX, a commercial finite element software, has been used to build a 3D numerical model to simulate these laboratory tests. This numerical model was used to provide confidence in the modelling approach, including the constitutive models used and the element types used for modelling the soil and the pipe. The length, width and height of the model were 5 m, 5 m and 5 m respectively. A trench with a width of 2 m was simulated in one direction across the model. The height of the trench was changed based on the backfill height, being equal to the backfill height plus the outer diameter of the pipe. The average element size of the pipe, trench and surrounding soil was 0.15 m, 0.15 m and 0.5 m, which is similar to a model developed previously by the authors to study the response of buried pipe under the BS traffic load (Alzabeebee et al., 2017; Alzabeebee et al., 2016). Four noded tetrahedron soil elements were used to model the trench and surrounding soil, while three noded shell elements were used to model the pipe. A

full bond has been considered between the soil and the concrete pipe. This assumption is valid because the deformation of the buried pipe is very small; hence the slippage between the pipe and the surrounding soil does not affect the accuracy of the soil-pipe interaction finite element modelling (Xu et al., 2017). In addition, previous studies have reported good predictions for the behaviour of buried pipes assuming a full bond between the soil and pipe (Mai et al., 2014; Meguid and Kamel, 2014; Alzabeebee et al., 2017; Xu et al., 2017). The finite element mesh is shown in Figure 2. A linear elastic model was used to simulate the behaviour of the pipe. This model was considered appropriate because the pipe did not experience any cracking and its response remained in the elastic zone under the full load of 100 kN (MacDougall, 2014). The soil was modelled using the Duncan-Chang hyperbolic soil model (Duncan and Chang, 1970). This model was used because it is capable of modelling the effect of stress level on the soil stiffness, which in turn provided a better prediction for the behaviour of the pipe (Dhar et al., 2004; Kang et al., 2007; Kang et al., 2008a,b; Kang et al., 2013a,b; Kang et al., 2014; Katona 2017; Kim and Yoo, 2005). The backfill height and the surrounding soil was simulated using poorly graded gravelly sand with a minimum degree of compaction of 90 % of the Standard Proctor test (GP90), while the soil in the haunch zone was simulated using sandy silt with a compaction degree of 90% (ML90). The hyperbolic material properties of the GP90 and ML90 soils were adopted from Boscardin et al. (1990) and are shown in Table 3. The modulus of elasticity (E_c) and the Poisson's ratio (υ) of the pipe were 38450896 kPa and 0.2, respectively. The elastic modulus of the concrete was calculated using Equation 3 (ACI, 2014).

$$E_c = 57000\sqrt{f_c'} \quad (3)$$

Three steps were performed to model the installation of the pipe and the loading:

Step 1: The initial soil stresses of the compacted material beneath the pipe were calculated using a coefficient of lateral soil pressure of 1.0 (Brown and Selig, 1991).

Step 2: The bedding soil, pipe and soil above the pipe were added, and the initial soil stresses were calculated using a coefficient of lateral soil pressure of 1.0 (Brown and Selig, 1991).

Step 3: A uniformly distributed surface load was applied in 25 equal loading increments.

Figures 3, 4 and 5 compare the calculated and measured bending moment in the pipe due to the backfill soil weight and traffic load with a backfill height of 0.3 m, 0.6 m and 0.9 m, respectively. It can be seen that the model predicts the bending moment with good accuracy for all of the backfill heights, bearing in mind the assumptions made in the modelling and the potential variability in the test results. The percentage difference between the maximum calculated and measured bending moment is 25 %, 10 %, and 15 % for backfill heights of 0.3 m, 0.6 m, and 0.9 m, respectively. Furthermore, the numerical model is able to predict the trend of the bending moment around the pipe. Hence, these results give confidence in the methodology adopted for the numerical modelling in the present study. Moreover, the developed model can be taken forward to investigate other scenarios of pipes with different diameters and thicknesses under shallow and deep burial conditions through an extensive parametric study.

Table 3: The material properties of the soil for the validation problem (Boscardin et al., 1990)

Property	GP90	ML90
γ (kN/m^3)	20.99	18.84
υ	0.3	0.3
c'(kPa)	1	24
ϕ'(°)	42	32
K	640	200
R_f	0.75	0.89
n	0.43	0.26

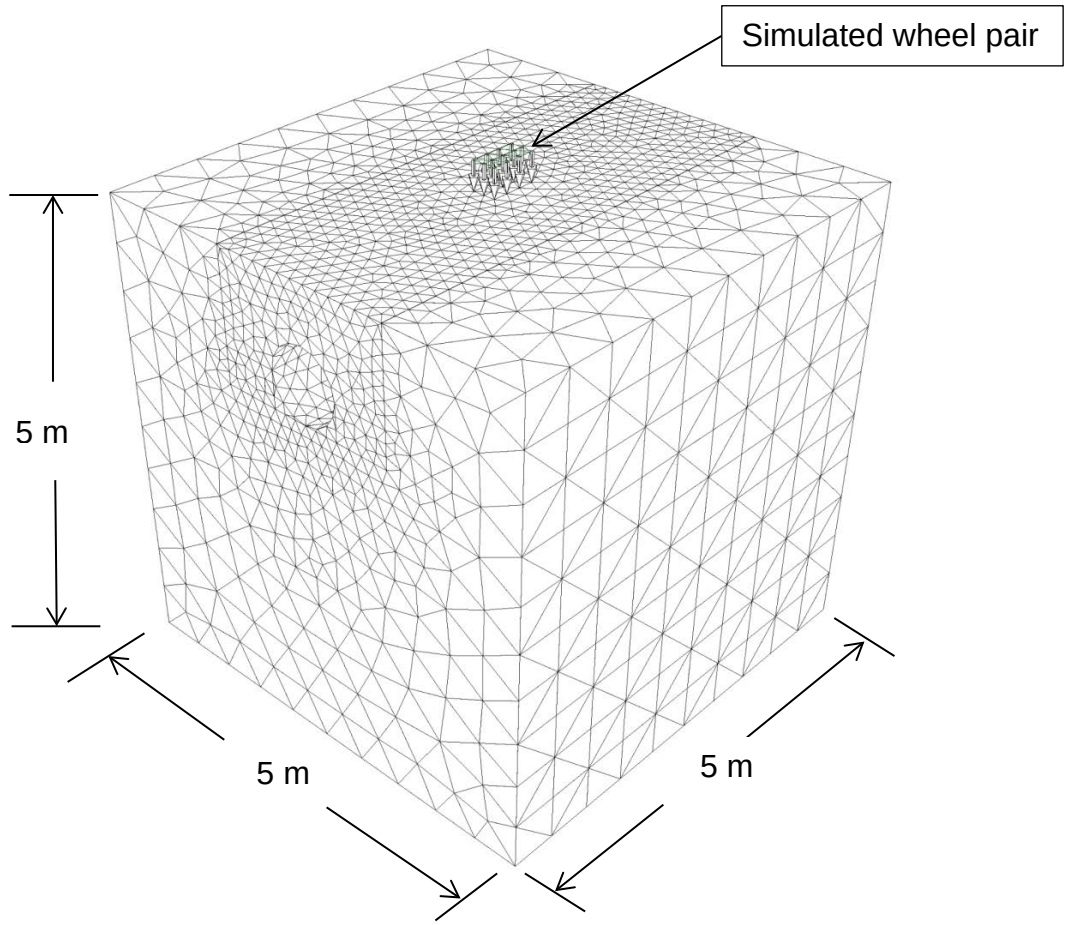

Figure 2: Finite element mesh used in the validation problem

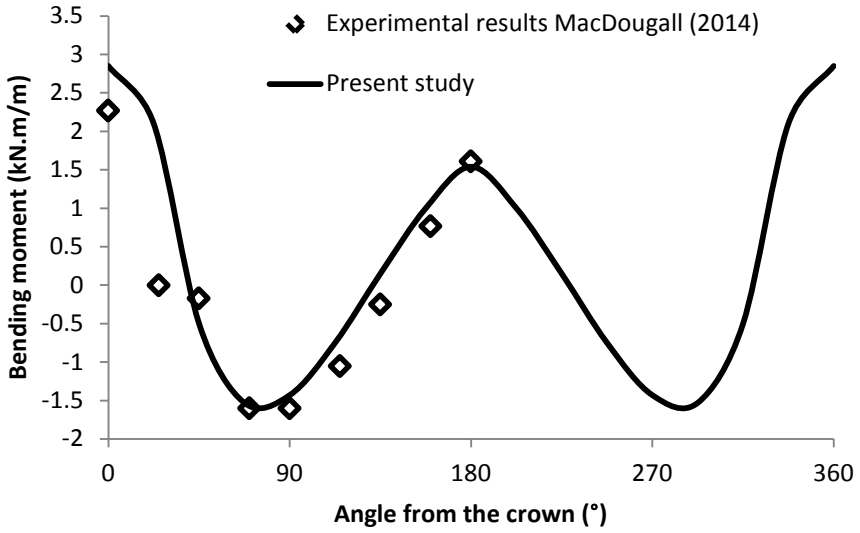

Figure 3: Bending moment in the concrete pipe under a combined load (soil weight and traffic load) with a backfill height of 0.3 m

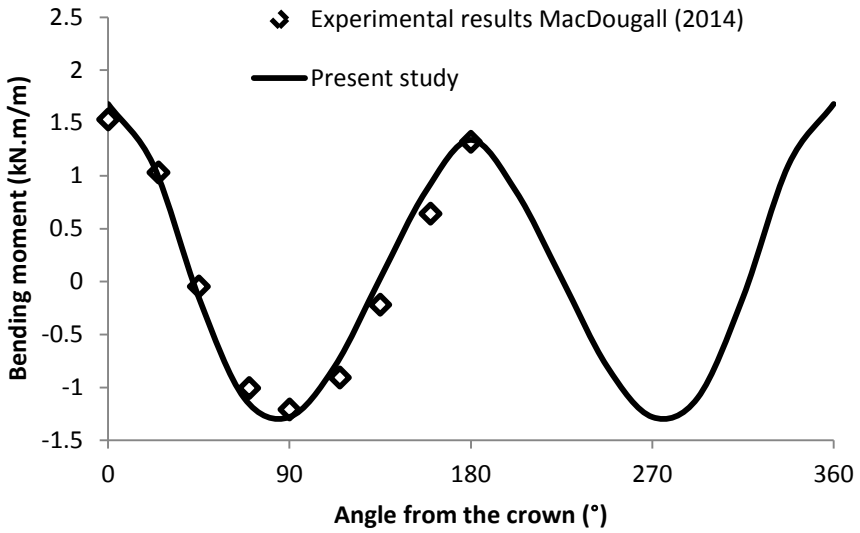

Figure 4: Bending moment in the concrete pipe under a combined load (soil weight and traffic load) with a backfill height of 0.6 m

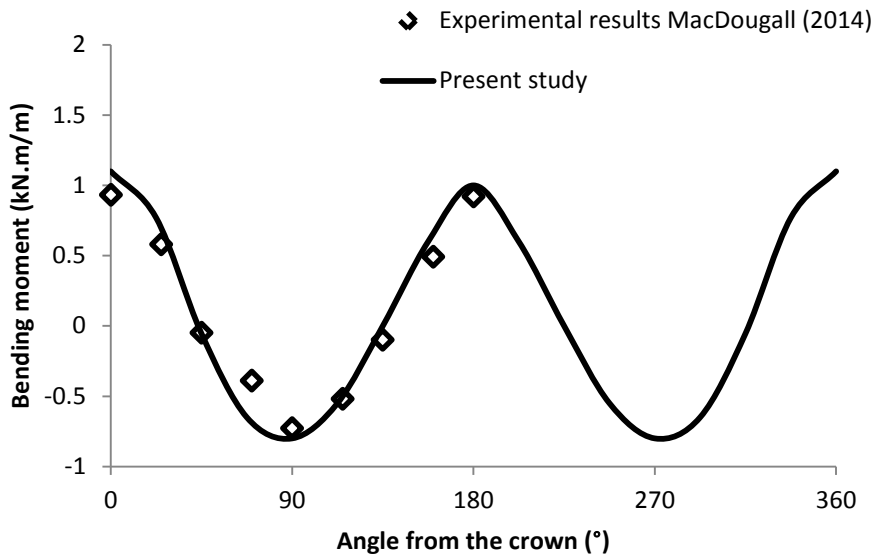

Figure 5: Bending moment in the concrete pipe under a combined load (soil weight and traffic load) with a backfill height of 0.9 m

4. Parametric study

A parametric study has been carried out to investigate the effect of backfill height, pipe diameter and pipe wall thickness on the bending moments developed in the pipe wall under soil loads, and hence the associated soil load bedding factor. The pipe diameters considered in this study are shown in Table 4. These diameters were considered to investigate the impact of the pipe diameter on the bedding factor and hence, implicitly the soil arching.

A maximum backfill height of 40 m has been considered in this study. This backfill height was considered necessary to provide a greater understanding of the effect of backfill height on the bending moment and the associated bedding factor. This also implicitly provides greater understanding of the soil arching effect, as previous studies have shown that vertical arching is significantly affected by the backfill height (Allard and El Naggar 2016; Kang et al., 2007). It should be noted that the backfill height has been taken down to a minimum of 1 m in this study, although it is

recognised at these lower backfill heights traffic loading (not considered in this paper) will be dominant in this region when the pipes are buried under trafficked areas. However, there are instances where pipes are laid under soil load only and the surface is not trafficked. Hence, the authors felt it is important to provide analyses, and hence the ability to determine bedding factors, for the full range of backfill heights (i.e. 1 m to 40 m). The backfill height was simulated by applying a uniformly distributed load to the top surface of the model. This technique has been successfully used by other researchers to simulate a pipe under increasing soil weight without the need to add more soil elements, which in turn significantly reduces the time to complete each analysis (Balkaya et al., 2012a,b; Balkaya et al., 2013; Dhar et al., 2004; Kang et al., 2007; Tan and Moore, 2007).

Furthermore, the four AASHTO installation types (Type 1, Type 2, Type 3 and Type 4) have been considered in the analysis by changing the degree of compaction and the type of soil in the haunch zone. It is worth mentioning here that in the AASHTO Type 1 installation the pipe is fully supported and hence it is equivalent to class S in the BS. In addition, in class F the pipe is partially supported in the haunch zone which is similar to Type 3. Furthermore, in class N and DD the pipe is directly installed on stiff soil, hence it is similar to AASHTO Type 4 installation. Finally, the minimum support condition of class B (i.e. BF = 1.9) can be considered similar to Type 2 where the pipe is well supported but not quite as well supported as for class S. Therefore, the cases considered in this study are also similar to the BS classes and hence the results are equally applicable to the BS classes.

It should be noted that the bedding soil beneath the pipe in these analyses has been modelled using a compacted well-graded sandy soil (SW) with a degree of compaction of 90% of the Standard Proctor maximum dry density for all of the

installation types (hereafter referred to as SW90). The assumption of a stiff bedding was made to simulate the worst case scenario since excavating the native soil under the pipe is a time consuming process and increases the installation cost by approximately 15% (Wong et al., 2006). Hence, it is expected that the pipe is laid directly on the stiff soil in practice (overconsolidated natural soil) and not following the AASHTO Standard of loose soil beneath the pipe for Type 1, Type 2 and Type 3 installation conditions. However, the full haunch zone has been modelled following the AASHTO recommendation with a SW95 soil for Type 1, SW90 soil for Type 2, ML90 (sandy silt) soil for Type 3 and ML49 soil for Type 4. The backfill soil was modelled using a SW90 soil for all of the cases. The soil parameters used in the analyses are shown in Table 5. It is important to mention that the assumption of thin shell theory has been employed (i.e. using shell elements to model the pipe) to add additional conservatism to the analysis, as the thin shell theory provides a higher bending moment than the thick ring theory with a percentage range from 2% to 10% (Moore et al., 2014). Hence, the bedding factor derived using this theory will be less than that derived following the thick shell theory.

The bedding factor (BF) has been calculated by dividing the maximum positive bending moment developed in the pipe wall during the three-edge bearing test, based on the force calculated using the AASHTO arching factors (Equation 5), by the maximum positive bending moment developed in the buried pipe (obtained from the numerical modelling), as shown in Equation 4 (Petersen et al., 2010; Young and O'Reilly, 1987). This approach has been adopted because the development of the crack in the concrete pipe wall is related to the development of the bending moment in the pipe wall, as the bending moment controls the design of buried pipes (i.e. it controls the tensile stresses in the pipe wall) (Tan and Moore, 2007).

$$BF = \frac{0.318 \times W_t \times r}{M} \quad (4)$$

$$W_t = VAF \times \gamma \times H \times D_{out} \quad (5)$$

Where, W_t is the calculated total force applied on the pipe, r is the radius of the pipe measured to the centre of the pipe wall, *M* is the bending moment of the buried pipe calculated from the finite element modelling, VAF is the vertical arching factor (VAF = 1.35 for Type 1, 1.4 for Type 2, Type 3 and 1.45 for Type 4 (AASHTO, 2016)), *H* is the backfill height, γ is the unit weight of the soil and D_{out} is the outside diameter of the pipe.

Table 4: Pipe diameters and wall thicknesses

Inside diameter (*D*) (m)	Wall thickness (*t*) (m)
0.3	0.055
0.6	0.094
1.2	0.144
2.4	0.229

Table 5: Material properties used in the parametric finite element analysis (Boscardin et al., 1990)

Property	SW95	SW90	ML90	ML49
γ (kN/m^3)	22.07	20.99	18.84	10.40
υ	0.3	0.3	0.3	0.3
c′ (kPa)	1	1	24	1
ϕ'(°)	48	42	32	23
K	950	640	200	16
R_f	0.7	0.75	0.89	0.55
n	0.6	0.43	0.26	0.95

4.1. Effect of backfill height

Figure 6a shows the effect of backfill height on the maximum bending moment developed in a pipe with an inside diameter of 0.3 m. As expected, increasing the backfill height increases the maximum bending moment due to the increase of the soil pressure. In addition, it can also be seen that changing the bedding type (i.e. the soil in the haunch zone) has a significant effect on the developed bending moment. For example, changing the bedding type from Type 1 to Type 2 increases the maximum bending moment by 19%, while changing the bedding type from Type 1 to Type 4 increases the bending moment by 62%. This increase is due to the concentration of the forces in the invert zone, which increases the maximum bending moment. This is because of the decrease in the mobilization of the haunch support as the compaction of the soil in the haunch zone decreases (Alzabeebee et al., 2016; Pettibone and Howard, 1967).

Figure 6b shows the calculated soil load bedding factor using Equation 4 for a pipe diameter of 0.3 m with different backfill heights and installation types. It can be seen that increasing the backfill height non-linearly increases the bedding factor. The non-linear behaviour is due to the decease of the negative arching as the backfill height increases and the use of a constant arching factor in the AASHTO equation to calculate the laboratory force (i.e. Equation 5). This is in agreement with the conclusions of Allard and El Naggar (2016) and Kang et al. (2007), where they also found that the negative vertical arching decreases as the backfill height increases. Furthermore, it can be seen that as the installation quality decreases, the bedding factor also decreases due to the significant increase in the bending moment as discussed in the previous section. However, the bedding factors for installation Type 1 are almost the same as for Type 2, with an average percentage difference of

1.45%. This is due to the use of a higher vertical arching factor in the laboratory force calculation for Type 2 installations (i.e. VAF = 1.4). This has eliminated the difference in the bending moment between Types 1 and 2 (i.e. 19%) and produced very similar values for the bedding factor.

It is also noted that after a backfill height of approximately 10 m, the bedding factors do not change significantly. This means that the negative soil arching does not significantly decrease after a backfill height of 10 m. In addition, Figure 6b shows that the support of the pipe has an effect on the soil arching since the rate of increase in the bedding factor for Types 1 and 2 was higher than that for Types 3 and 4 after a backfill height of 10 m.

Figures 6c and d shows the ratio of the bedding factor obtained from the present study to the design bedding factors adopted in the AASHTO standard and BS, respectively. The AASHTO bedding factors were calculated from Table 1 depending on the diameter of the pipe and the installation condition. Similarly, for the BS, the bedding factors were calculated from Table 2 depending on the installation condition. However, the minimum values (2.2 for class S, 1.9 for class B, 1.5 for class F and 1.1 for class N) were used as the numerical modelling simulated the worst case scenario. It can be seen that for both standards the bedding factors adopted are conservative except for the AASHTO standard for Type 1 installation, where the ratio is less than 1. Furthermore, it can be seen that the degree of conservatism of both design standards increases as the backfill height increases or as the installation quality decreases. However, for Type 3 and 4 installations, the ratio stabilises after approximately 15 m of backfill height.

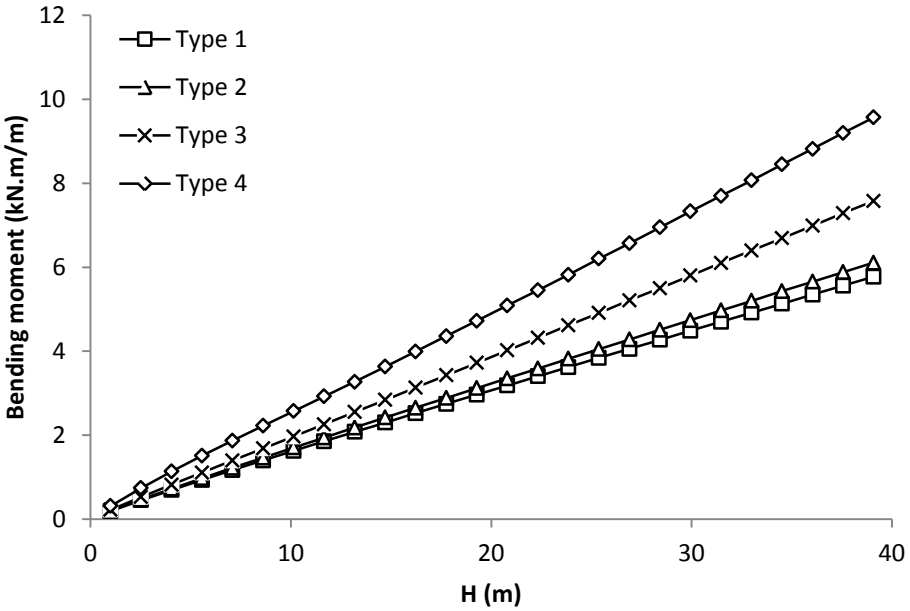

Figure 6a: Effect of the backfill height on the developed bending moment for a pipe with a diameter of 0.3 m buried in different installation conditions

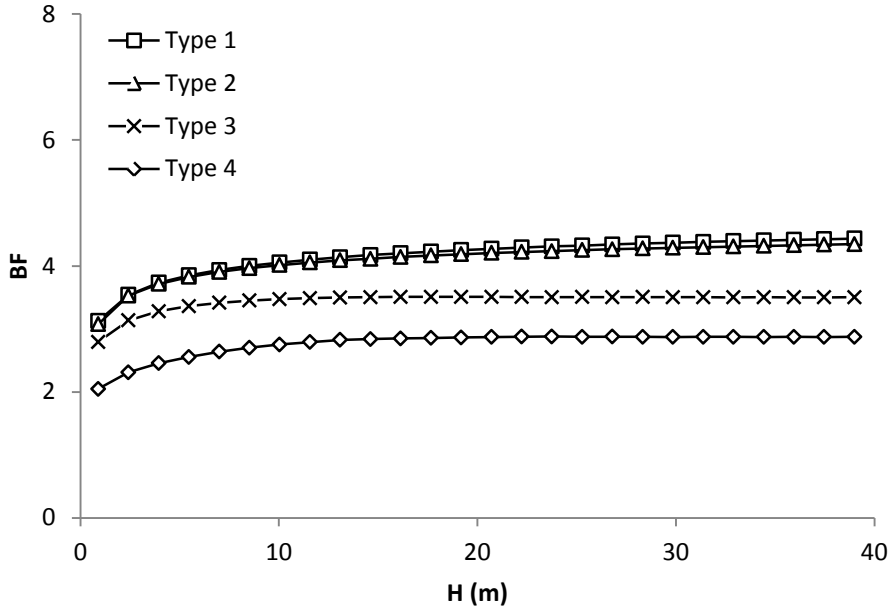

Figure 6b: Effect of backfill height on the soil load bedding factor for a pipe diameter of 0.3 m buried in different installation conditions

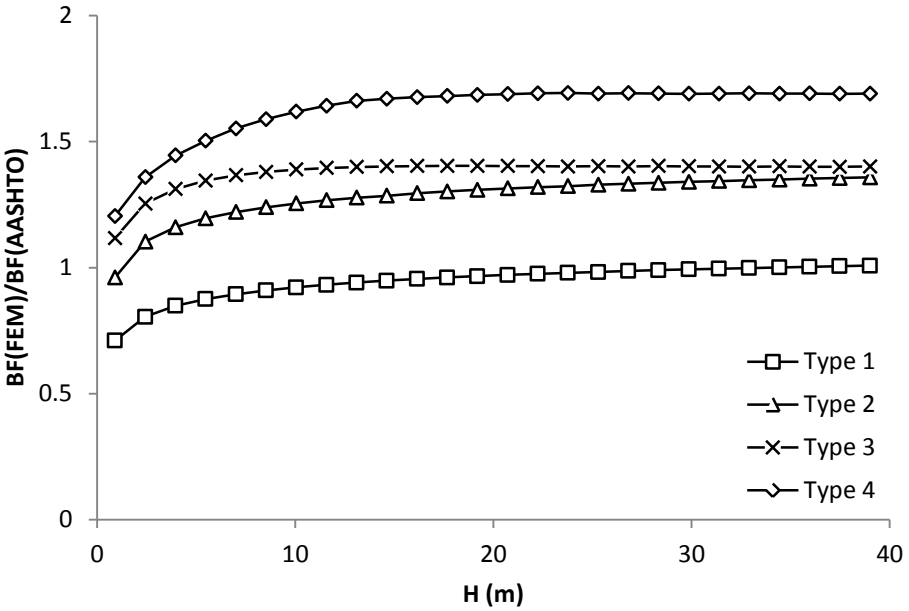

Figure 6c: Ratio of bedding factors obtained from the numerical modelling and the AASHTO standard values (pipe diameter 0.3 m)

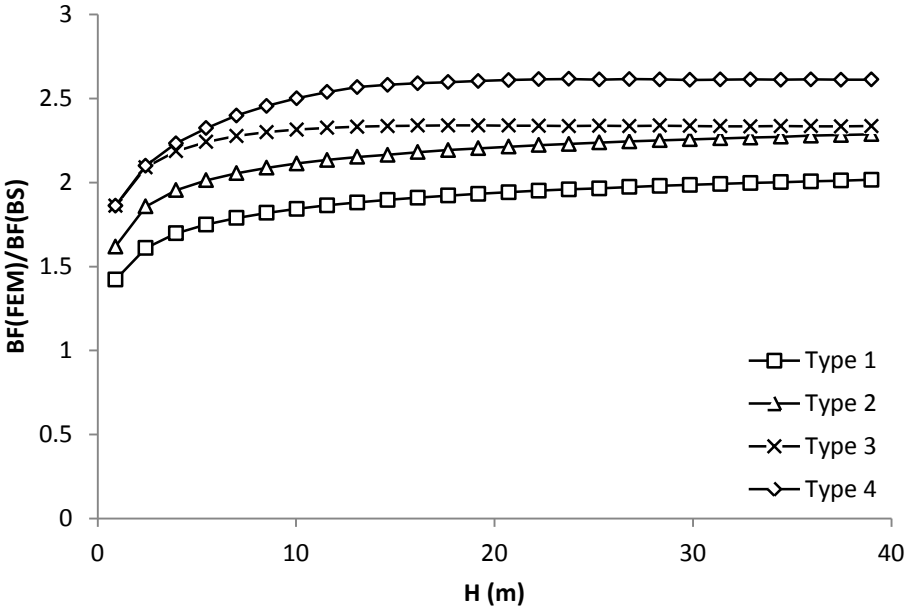

Figure 6d: Ratio of bedding factors obtained from the numerical modelling and the BS values (pipe diameter 0.3 m)

4.2. Effect of pipe diameter

Figure 7a shows the effect of the pipe diameter on the maximum bending moment developed for the buried pipes installed using a Type 1 installation condition. It can be seen that, as expected, increasing the diameter of the pipe significantly increases the bending moment. The average percentage increase in the maximum bending moment is equal to 240%, 1013% and 4237% as the diameter changes from 0.3 m to 0.6 m, 1.2 m and 2.4 m, respectively. This is because of the increase in the soil pressure at the invert of the pipe as the diameter of the pipe increases due to the increase of the backfill height above the invert, and hence due to the larger span (pipe diameter), the bending moment increases (Wang et al., 2006).

Figure 7b shows the effect of the pipe diameter on the calculated soil load bedding factor. It can be seen that there is a complex interaction between bedding factor and diameter and backfill height over the first 16 m, after which the relationships stabilize. This behaviour is due to the over simplification in the analytical method adopted in the design standards for calculating the soil force applied on the pipe. The method takes the horizontal projection of the pipe and assumes that the pipe is a rectangular culvert and uses a constant vertical arching factor derived from the pipe thrust at the springline. As a result, the force applied on the pipe calculated in the laboratory and used to calculate the laboratory bending moment term in Equation 4 (i.e. $0.318\, W_t\, r$) increases significantly as the diameter of the pipe increases. Taking this into account together with the change in arching and the increase in the soil pressure as the backfill height and the diameter increase, produces these complex relationships.

Figures 7c and d show the ratio of the bedding factor obtained from the present study to the design bedding factor adopted in the AASHTO standard and BS for pipes buried using a Type 2 installation, respectively. It can be seen from Figure 7c

that the AASHTO bedding factors are conservative except for a pipe with an inside diameter of 2.4 m buried with a backfill height less than 2 m. Figure 7d shows that the BS bedding factors are conservative for all cases. Furthermore, it can also be seen from both Figures that increasing the backfill height increases the degree of conservatism (although for the smaller diameter pipes the value does not increase significantly after approximately 15 m of backfill height). This is due to the independency of the bedding factors adopted in both standards on the backfill height. In addition, Figure 7c shows that the ratio between the bedding factor obtained from the numerical modelling to the AASHTO bedding factor is equal to 1.71 for a pipe with an inside diameter of 0.6 m and a backfill height of 20.3 m. This is in good agreement with the ratio (experimental bedding factor to the AASHTO bedding factor) reported by MacDougall et al., (2016) from the experimental study (reported earlier) on a pipe with the same dimensions (diameter and thickness) and backfill height, where the calculated ratio was 1.77 (i.e. percentage difference 3.4%).

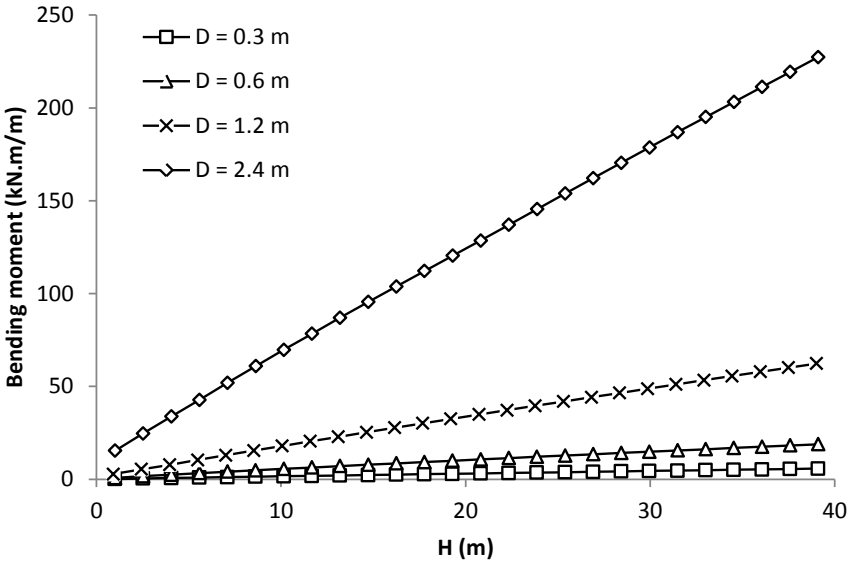

Figure 7a: Effect of pipe diameter on the maximum bending moment developed in the buried pipes installed using the AASHTO Type 1 installation

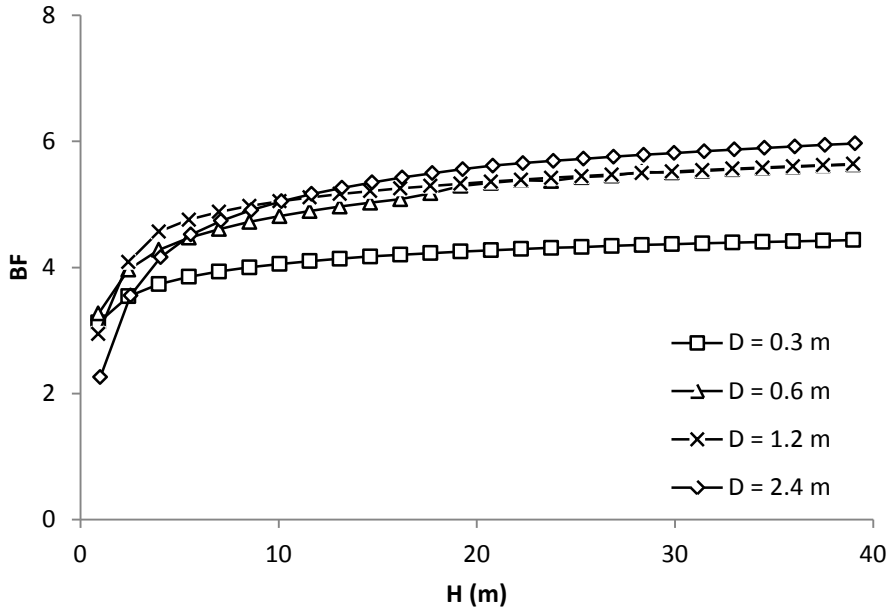

Figure 7b: Effect of pipe diameter on the calculated soil load bedding factor for buried pipes installed using the AASHTO Type 1 installation

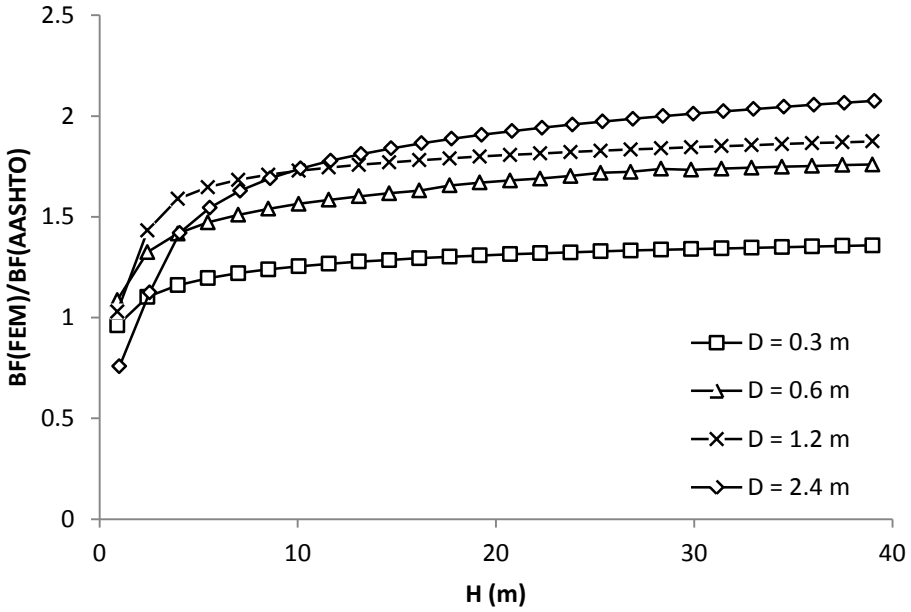

Figure 7c: Ratio of bedding factor obtained from the numerical modelling and the bedding factor from the AASHTO design standard for pipes buried using a Type 2 installation

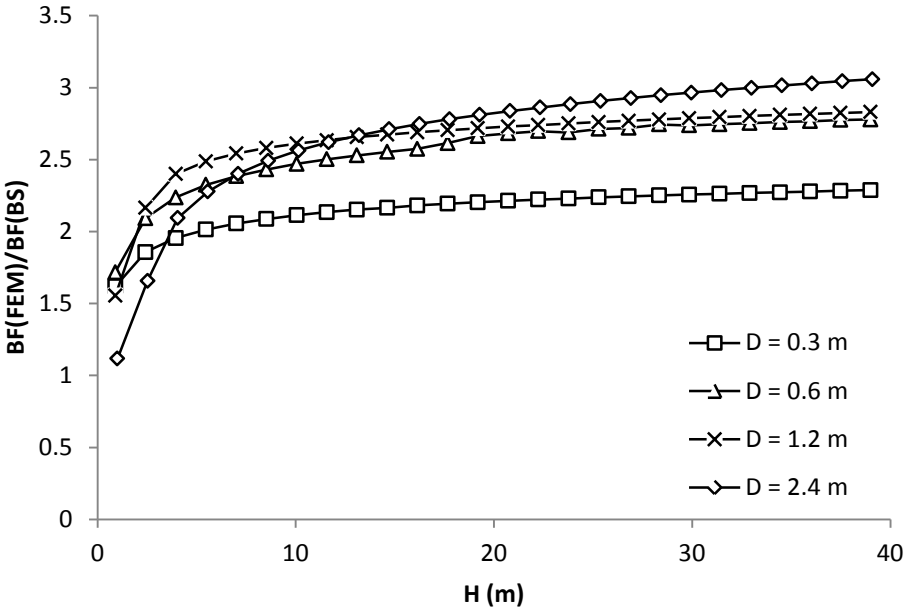

Figure 7d: Ratio of bedding factor obtained from the numerical modelling and the bedding factor from the BS for pipes buried using a Type 2 installation

4.3. Effect of pipe thickness

To investigate the effect of the pipe wall thickness, additional finite element models were built with two additional wall thicknesses, one was equal to half of the original thickness (shown in Table 4) and the other was assumed to be double the original thickness. This was done to provide a general understanding of the bending moments and also to demonstrate the dependency of the calculated bedding factor on changes in wall thickness. Figure 8a shows the maximum bending moment for a 2.4 m diameter pipe with different wall thicknesses buried using a Type 1 installation condition. It can be seen that doubling the wall thickness of the pipe increases the maximum bending moment by 73%, while decreasing the pipe wall thickness by half decreases the maximum bending moment by 61%. The increase in the bending moment can be explained by the concept of soil arching, where increasing the wall thickness of the pipe increases the pipe stiffness, which consequently increases the

negative arching meaning that the soil pressure attracted by the pipe will be increased (Kang et al., 2007; Moore, 2001), and hence this induces a larger bending moment.

Figure 8b shows the soil load bedding factor calculated from the maximum bending moment values. The Figure shows that the bedding factor values is affected by the wall thickness of the pipe, whereby increasing the wall thickness decreases the bedding factor due to an increase in the field bending moment (i.e. the bending moment from the finite element modelling). This Figure also indicates that the design standards should consider the pipe thickness when calculating the bedding factor to ensure a robust design.

In summary, the parametric study has shown that the BS bedding factors are very conservative, where the ratio of the bedding factors obtained from the finite element modelling to the design standard bedding factors ranged from 1.03 to 3.08.For the AASHTO standard the bedding factors are not safe for shallow depths, but become increasingly more conservative as the backfill height increases, where the ratio of the bedding factors obtained from the numerical modelling to the design standard bedding factors ranged from 0.61 to 2.08. Furthermore, the results have shown that the bedding factor is significantly affected by the diameter of the pipe, the backfill height and the wall thickness of the pipe. Therefore, to achieve a robust design, the designer should consider all of these parameters.

In order to make the results from this study more useful for pipe designers, an advanced data mining technique (evolutionary polynomial regression) has been employed to derive explicit and concise models for the bedding factors for each installation type. This technique is capable of modelling highly complex relationships

with high accuracy (Ahangar Asr and Javadi, 2016; Alani et al., 2014; Faramarzi et al., 2012; Faramarzi et al., 2014; Faramarzi et al., 2013; Javadi et al., 2012; Savic et al., 2006). The decision to use this technique was made because of the highly complex behaviour of the bedding factor and its interaction with the parameters discussed earlier. Furthermore, an attempt was made to use classical non-linear analysis to obtain correlations, however this resulted in poor accuracy. Details of the evolutionary polynomial regression and the modelling steps are described in detail in the following sections.

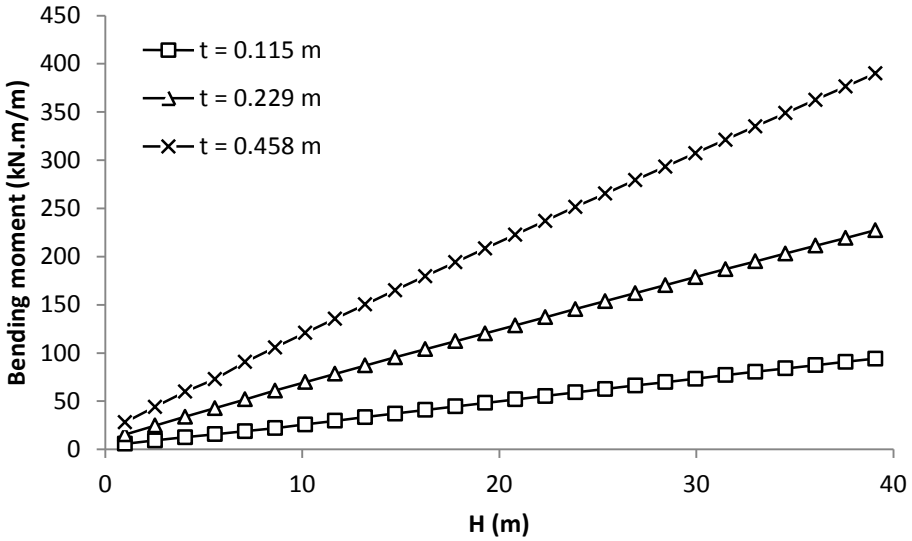

Figure 8a: Effect of pipe wall thickness on the maximum bending moment developed for buried pipes installed using the AASHTO Type 1 installation

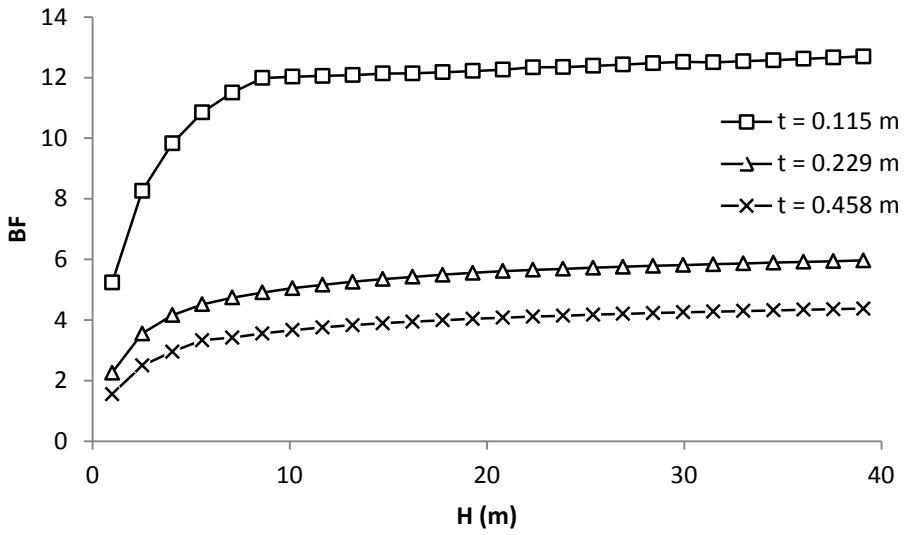

Figure 8b: Effect of pipe wall thickness on the calculated soil load bedding factor for buried pipes installed using the AASHTO Type 1 installation

5. Development of the model

5.1. The EPR method

Evolutionary polynomial regression (EPR) is a hybrid data mining technique based on artificial intelligence and is capable of modelling complex non-linear problems (Giustolisi and Savic, 2006). EPR combines a genetic algorithm with the least squares method to search for the best polynomial model to fit the input and output data (Giustolisi and Savic, 2006; Giustolisi and Savic, 2009).

EPR searches for the best fit relationship by changing the combination of exponents defined by the user. This search is conducted using a genetic algorithm (more details can be found in Giustolisi and Savic, 2006; Giustolisi and Savic, 2009). EPR picks the best mathematical expression by calculating the coefficient of determination (CD) (Equation 6) for each mathematical expression and chooses the equation which achieves the highest CD value (Alani et al., 2014; Faramarzi et al., 2014).

$$CD = 1 - \frac{\sum_N (Y_a - Y_p)^2}{\sum_N (Y_a - \frac{1}{N}\sum_N Y_p)^2} \quad (6)$$

Where Y_a is the dependent input values, Y_p is the calculated dependent input values from the EPR model and N is the number of the data points.

5.2. Modelling the bedding factor

As demonstrated in section 4, the calculated soil load bedding factor is significantly affected by the wall thickness of the pipe (t), the inside diameter of the pipe (D) and the backfill height (H) for all the installation types considered. This means that incorporating all of these parameters into the resulting model is necessary to achieve a robust and economical concrete pipe design.

For each installation type a total number of 312 points were obtained from the finite element modelling for different diameters, backfill heights and thicknesses. All of these data were used in the training and testing of the models. It is common in artificial intelligent techniques to divide the data into two sets. One set is used for training the model and the other set is used for validating the capabilities of the developed model (Alani et al., 2014). This procedure is usually considered because these modelling techniques are not simple curve fitting exercises and they search for the best solution by training the model. Hence, the model should be validated using unseen data in order to assess the reliability of the developed model and evaluate its ability to capture the trends in the data. In addition, the general statistical characteristics of the training and validation data should be similar to avoid model extrapolation (Alani et al., 2014). Therefore, in the present study the data were randomly shuffled and divided into a training set with 80% of the data and a validation set with 20% of the data. A statistical analysis was conducted after

completing the random shuffle to make sure that the training and validation data were comparable, which in turn provided a robust and representative model. Table 6 shows the minimum (Min), maximum (Max), mean (mean) and the standard deviation (STDV) values for the training, the validation and all the data sets used in the EPR modelling for each installation type.

The EPR analysis started after completing the preparation of the training and validation data. In order to find the best mathematical expression, different exponent ranges, function types and numbers of terms were tested. As mentioned in the previous section, the EPR searches for the best mathematical expression by changing the exponent of the parameters used and solves the overdetermined system using the least squares method. The accuracy of the mathematical expression at each step was measured by calculating the CD. As the number of evolutions increased, the EPR learnt the best arrangement of the exponents and selected the best solution based on the calculated CD value. At the end of the analysis, the EPR provided different models with different numbers of terms. However, increasing the number of terms increases the model complexity and the risk of overfitting. In addition, providing a simple model is better from a practical point of view. Therefore, an effort was made to select the simplest model which captures the trend behaviour with the minimum percentage error for all of the considered diameters without significantly affecting the accuracy. This has been done by comparing the results of the EPR model with 2 terms, 3 terms, 5 terms, 6 terms and 7 terms and the finite element results, and applying the aforementioned criteria (i.e. model simplicity, trend behaviour and percentage error). Equations 7 to 10 show the chosen models from the EPR analysis for installation Type 1, Type 2, Type 3 and Type 4, respectively.

$$BF = -11.72\ \frac{t^2}{D^2} - 0.0037\frac{D}{t^2} - 1.05\frac{D}{\sqrt{t}\sqrt{H}} + 0.0206\frac{D^2}{t^2} + 5.14 \quad (7)$$

$$BF = -11.72\ \frac{t^2}{D^2} - 0.0037\frac{D}{t^2} - 1.05\frac{D}{\sqrt{t}\sqrt{H}} + 0.0202\frac{D^2}{t^2} + 5.14 \quad (8)$$

$$BF = -2.82\frac{t}{D\sqrt{H}} - 0.003\frac{D}{t^2} + 0.0195\frac{D^2}{t^2} - 0.13\frac{D^2}{t\sqrt{H}} + 3.4 \quad (9)$$

$$BF = -1.09\ \frac{1}{\sqrt{H}} + 0.0077\ \frac{D^2}{t^2} - 0.059\frac{D^2}{t\sqrt{H}} + 2.74 \quad (10)$$

Figures 9 a, b, c and d shows the EPR prediction (i.e. Equations 7, 8, 9 and 10) for the training and validation data in comparison with the finite element results. In addition, the coefficient of determination (CD) values obtained for the training and validation data are shown in Table 7. It can be seen from Figure 9 and Table 7 that the EPR predicts the bedding factor with a very good accuracy for all of the installation types.

It should be noted that the use of the developed models is straight forward. The designer can calculate the bedding factor based on the pipe diameter (which is usually calculated based on the flow requirements) and the backfill height (which is usually calculated based on the design slope of the pipes in the network). Therefore, the designer can assume a reasonable pipe wall thickness (obtained from pipe manufacturer specifications) and then calculate the required bedding factor. Finally, the required pipe capacity can be calculated using the obtained bedding factor.

Importantly, it should be noted here that the models were trained and tested with the data range provided from the finite element analysis (i.e. a diameter ranging from 0.3 m to 2.4 m and a backfill height ranging from 1 m to 40 m). Therefore, these models are only applicable to pipes with similar diameters and backfill heights used in the

current study and without the effect of the traffic load. Any attempts to use the model outside this range may result in a significant error.

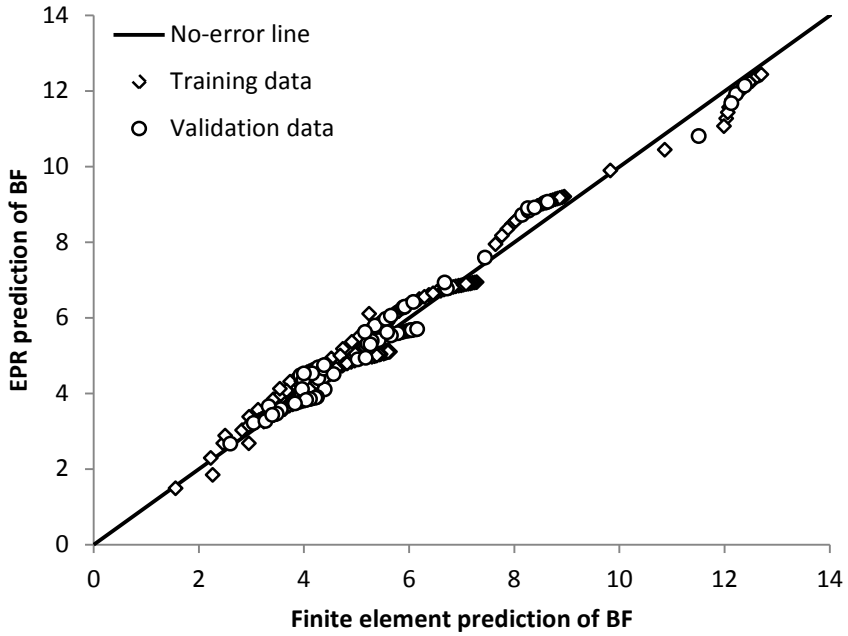

(a)

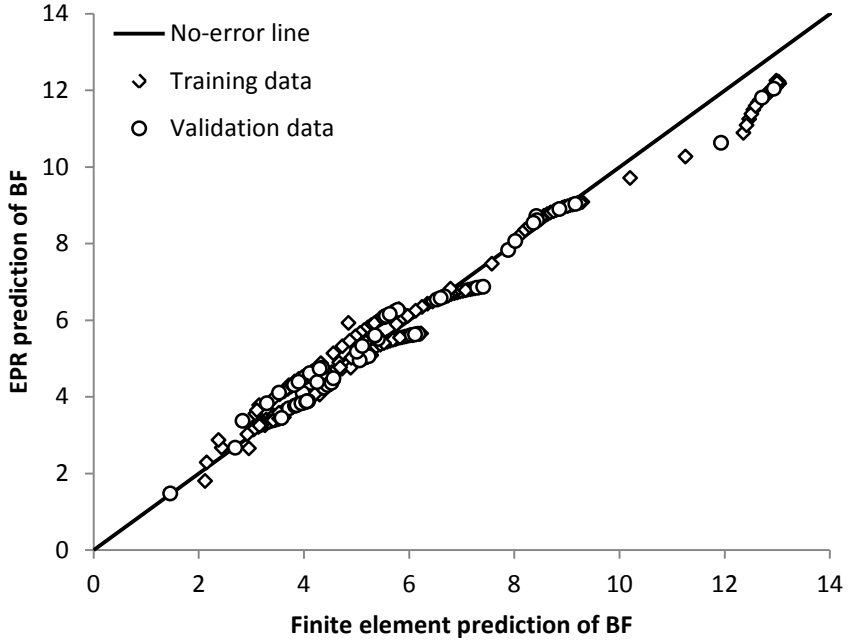

(b)

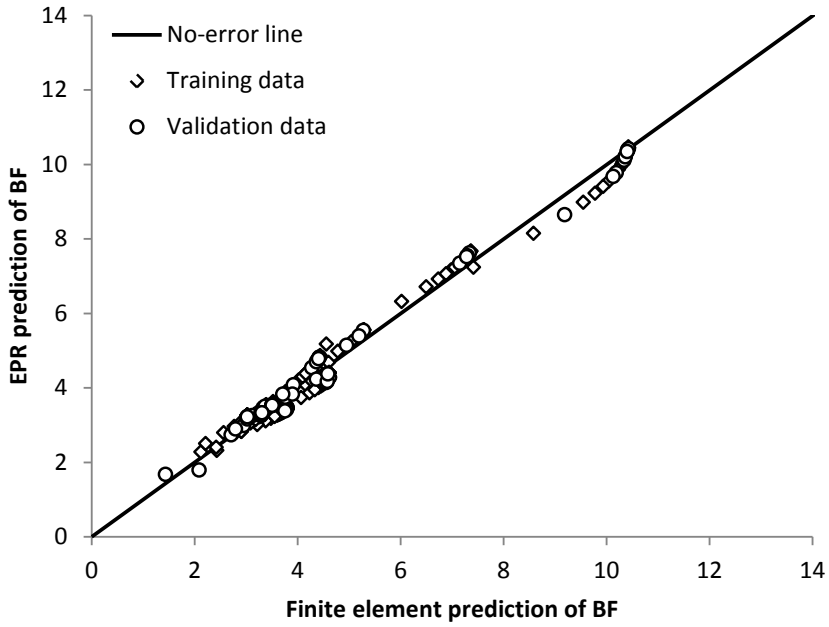

(c)

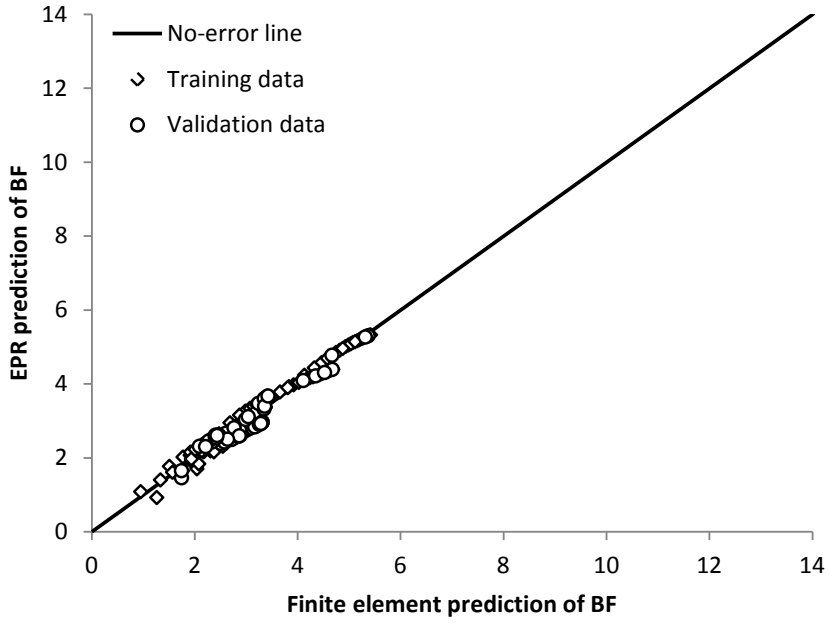

(d)

Figure 9: EPR calculated soil load bedding factors compared to the finite element results: (a) installation Type 1; (b) installation Type 2; (c) installation Type 3; (d) installation Type 4

Table 6: Statistics for the data used in the EPR analysis

		Type 1				Type 2				Type 3				Type 4			
		D (m)	t (m)	H (m)	BF	D (m)	t (m)	H (m)	BF	D (m)	t (m)	H (m)	BF	D (m)	t (m)	H (m)	BF
Training	Mean	1.15	0.15	20.56	5.67	1.13	0.15	19.76	5.58	1.15	0.15	19.40	4.77	1.11	0.15	20.16	3.02
data	Min	0.30	0.03	0.90	1.55	0.30	0.03	0.90	1.46	0.30	0.03	0.90	1.44	0.30	0.03	0.90	0.96
	Max	2.43	0.46	39.10	12.70	2.43	0.46	39.10	13.04	2.43	0.46	39.10	10.43	2.43	0.46	39.10	5.42
	STDV	0.82	0.12	11.30	2.35	0.82	0.12	11.37	2.46	0.83	0.12	11.54	1.87	0.81	0.12	11.40	0.79
Validation	Mean	1.08	0.15	17.77	5.32	1.14	0.15	20.98	5.70	1.08	0.14	22.43	4.53	1.23	0.16	19.36	2.99
data	Min	0.30	0.03	0.90	2.22	0.30	0.03	0.90	2.12	0.30	0.03	1.00	2.12	0.30	0.03	1.00	1.27
	Max	2.43	0.46	39.09	12.34	2.43	0.46	39.10	12.99	2.43	0.46	39.09	10.43	2.43	0.46	39.10	5.37
	STDV	0.80	0.12	11.87	2.26	0.82	0.12	11.81	2.57	0.78	0.11	10.83	2.08	0.84	0.13	11.70	0.73
All data	Mean	1.13	0.15	20.01	5.56	1.13	0.15	20.01	5.60	1.13	0.15	20.01	4.60	1.13	0.15	20.01	3.01
	Min	0.30	0.03	0.90	1.55	0.30	0.03	0.90	1.46	0.30	0.03	0.90	1.44	0.30	0.03	0.90	0.96
	Max	2.43	0.46	39.10	12.70	2.43	0.46	39.10	13.04	2.43	0.46	39.10	10.42	2.43	0.46	39.10	5.42
	STDV	0.82	0.12	11.45	2.33	0.82	0.12	11.45	2.48	0.82	0.12	11.45	1.92	0.82	0.12	11.45	0.78

Table 7: Coefficient of determination (CD) for the training and validation data (%)

Data set	Type 1	Type 2	Type 3	Type 4
Training	97.81	97.70	97.68	96.00
Validation	97.40	97.90	98.56	96.32

5.3. Sensitivity analysis

In this section, the results of a sensitivity analysis are presented to show the performance of the developed models. The aim is to illustrate that these models are able to predict the complex trend behaviour of the soil load bedding factor which has been presented and discussed in the parametric study section. Figure 10 shows the effect of the backfill height and installation condition on the calculated bedding factor using the developed models for the case of a pipe with an inside diameter of 1.2 m and a thickness of 0.144 m. It can be seen that the models are able to show the effect of the backfill height and the installation condition on the bedding factor, which has been discussed in section 4.1. Figure 11 (a, b, c and d) shows the effect of the pipe diameter on the bedding factor. Again, the results show that the developed models can capture the complex interaction of the bedding factor values as the diameter changes for all of the installation conditions. Figure 12 (a, b, c and d) shows the effect of the pipe thickness on the calculated bedding factor values for all of the installation conditions. The results clearly illustrate the ability of the developed model to capture the trend behaviour of the bedding factor as the thickness of the pipe changes.

In summary, these results give additional confidence in the validity of the models and hence these models can be recommended to use in the design practice.

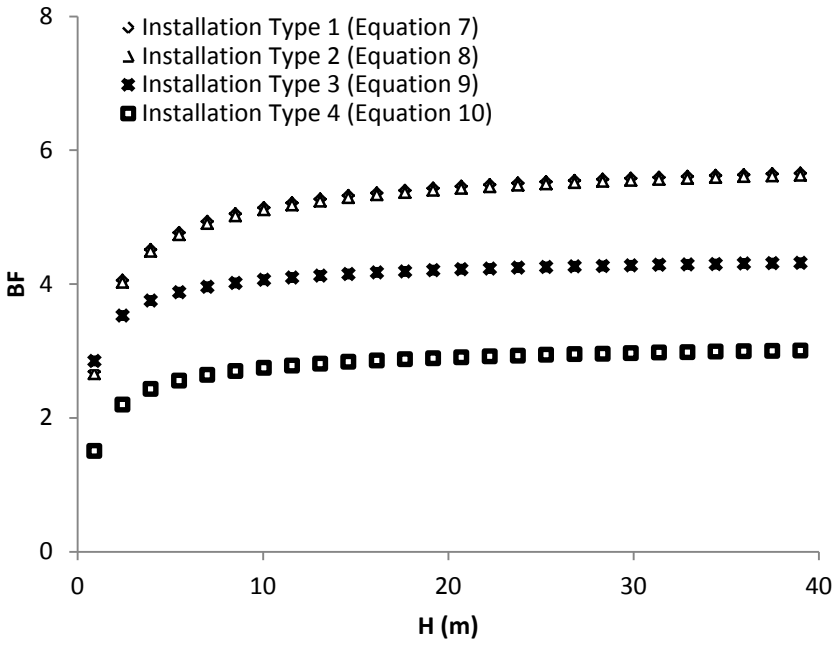

Figure 10: Effect of the backfill height on the calculated bedding factor

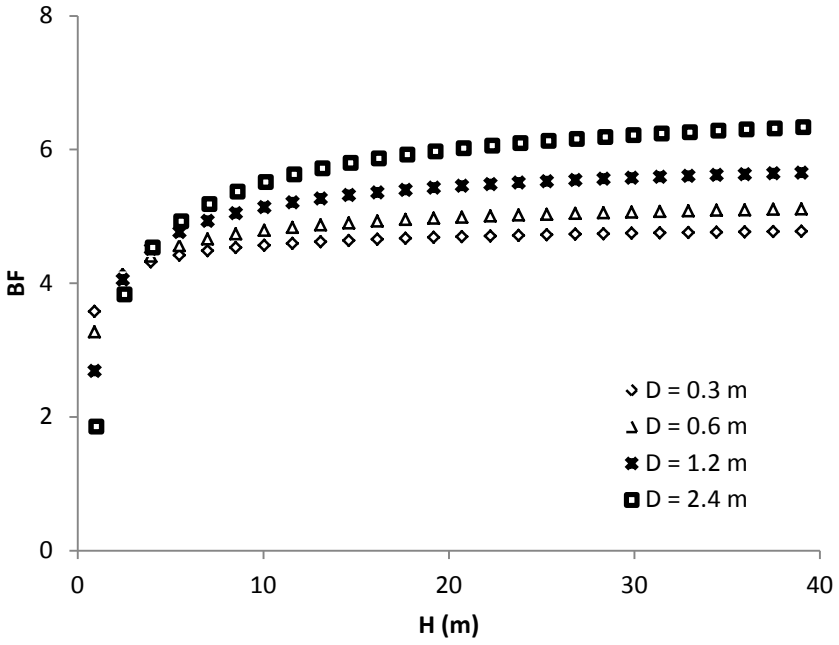

(a)

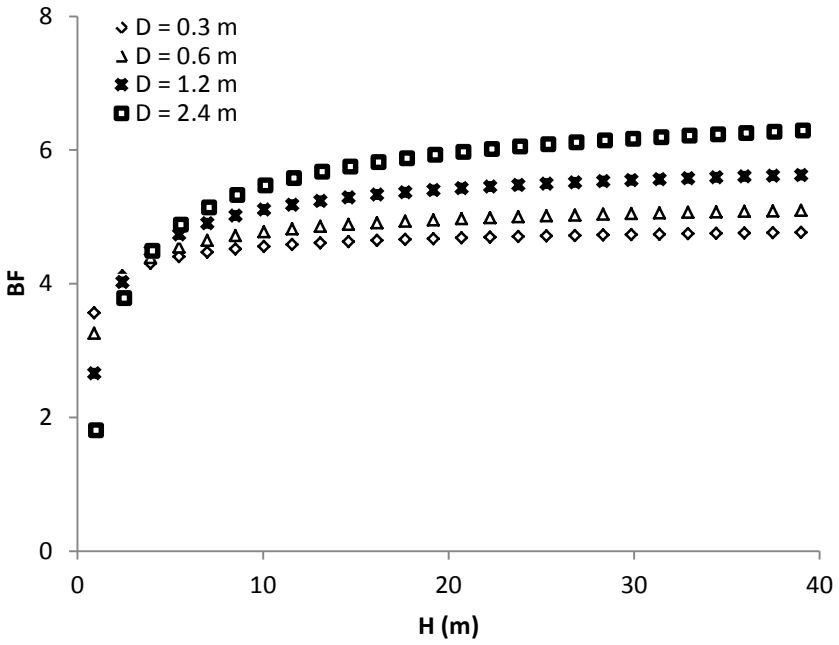
D = 0.3 m
D = 0.6 m
D = 1.2 m
D = 2.4 m
BF
H (m)
0
2
4
6
8
0
10
20
30
40

(b)

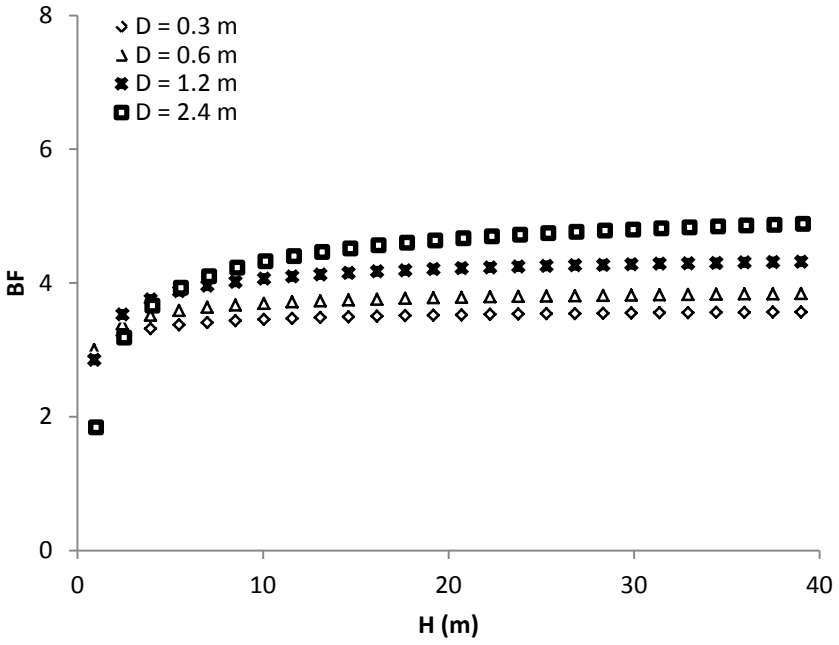
D = 0.3 m
D = 0.6 m
D = 1.2 m
D = 2.4 m
BF
H (m)
0
2
4
6
8
0
10
20
30
40

(c)

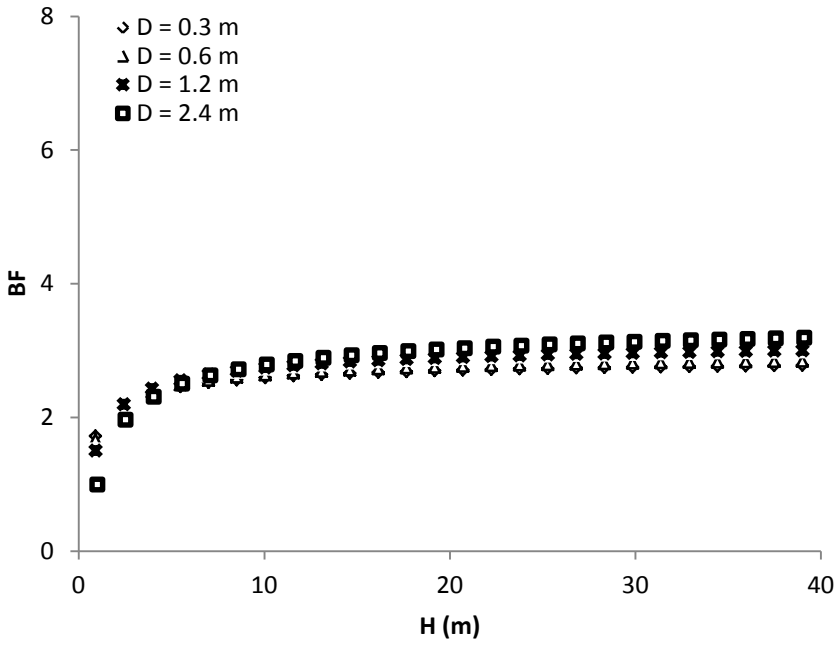

(d)

Figure 11: Effect of pipe diameter on the calculated soil load bedding factor: (a) Type 1 (Equation 7); (b) Type 2 (Equation 8); (c) Type 3 (Equation 9); (d) Type 4 (Equation 10)

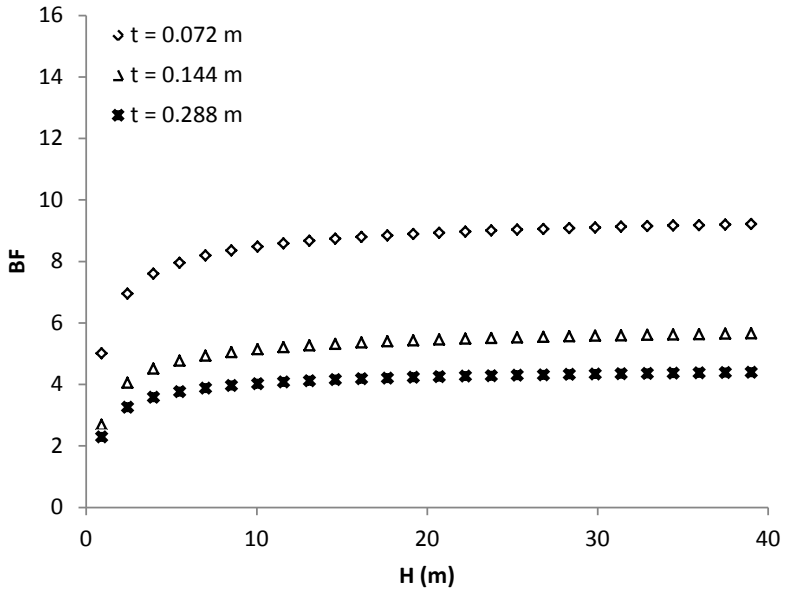

(a)

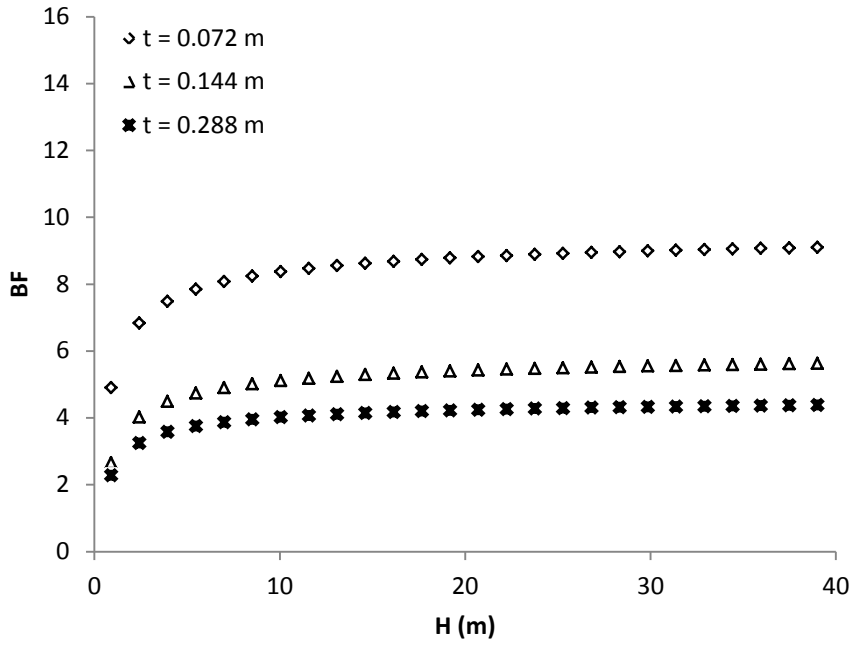
t = 0.072 m
t = 0.144 m
t = 0.288 m
BF
H (m)
0
2
4
6
8
10
12
14
16
0
10
20
30
40

(b)

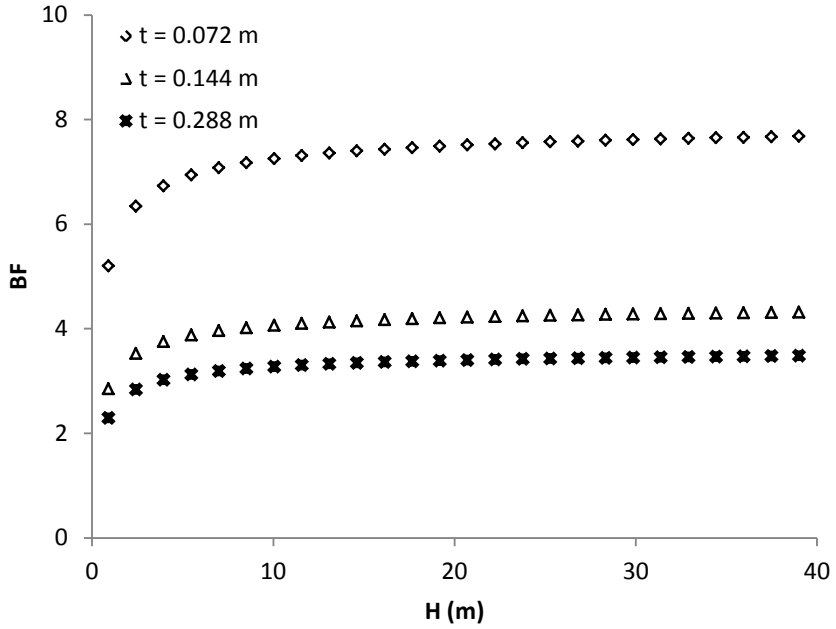
t = 0.072 m
t = 0.144 m
t = 0.288 m
BF
H (m)
0
2
4
6
8
10
0
10
20
30
40

(c)

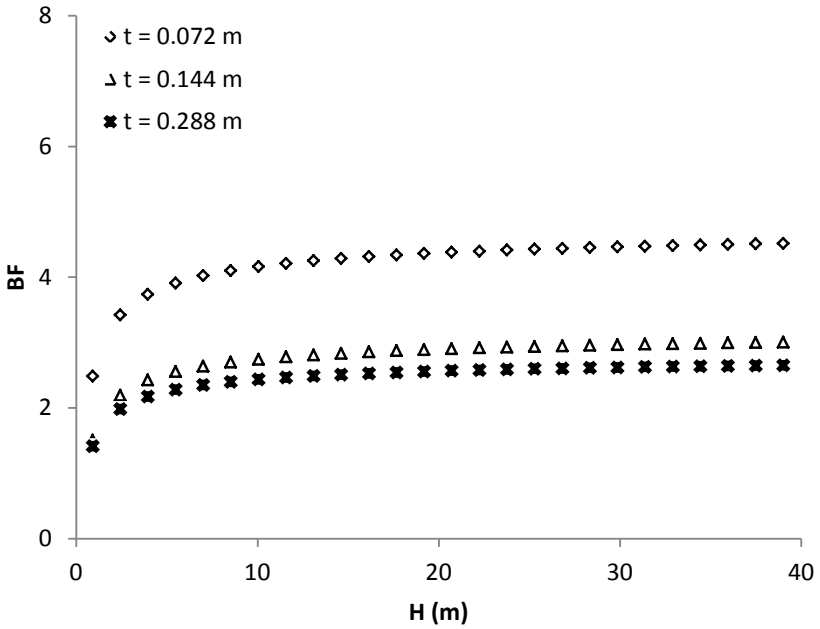

(d)

Figure 12: Effect of pipe thickness on the calculated soil load bedding factor: (a) Type 1 (Equation 7); (b) Type 2 (Equation 8); (c) Type 3 (Equation 9); (d) Type 4 (Equation 10)

5.4. Comparison with previous studies

As mentioned in the introduction, only one study has reported the soil load bedding factor of a concrete pipe buried under deep soil fill (MacDougall et al., 2016). MacDougall et al. (2016) tested a buried concrete pipe under deep soil fill using a biaxial test cell. The pipe used had an inside diameter of 0.6 m and a wall thickness of 0.094 m. MacDougall et al. (2016) tested the pipe by applying a uniformly distributed load to simulate the deep soil fill in the biaxial cell. The pipe was installed using a Type 2 installation. The strain in the pipe and the developing crack width in the pipe wall were monitored during the test and the pipe tested until it reached the failure limit (i.e. a crack width of 0.254 mm). The bedding factor was found to be 5.3 at a backfill height of 20.3 m.

In this section, the capabilities of the model developed for the bedding factor corresponding to a Type 2 installation (Equation 8) was tested by comparing the model prediction with the experimental bedding factor reported by MacDougall et al., (2016). The pipe geometric properties and backfill height reported by MacDougall et al., (2016) were used in the prediction. The calculated bedding factor using Equation 9 was equal to 5.0. Hence, the result from the model is in excellent agreement with the experimental bedding factor with a percentage difference of 5.7%. This comparison gives additional validation for the methodology adopted in this paper. The proposed models for the bedding factor can therefore be used with confidence in practice for achieving an economic pipe design, relative to the conservative values obtained from the current design AASHTO standard and the BS. In addition, the models proposed here can easily be applied to any pipe wall thickness. This is very useful if the designer wants to use a pipe with non-standard thickness (i.e. different from the AASHTO recommended thicknesses for different pipe classes).

6. Conclusion

A validated finite element model has been developed and used to investigate the effect of the installation type, pipe diameter, pipe wall thickness and backfill height on the maximum bending moment developed in buried concrete pipes. The maximum bending moment obtained from these analyses has been used to calculate the soil load bedding factor and the results have been compared to the BS and AASHTO standard recommended bedding factors. The following conclusions can be drawn from the present study:

1- The maximum bending moment developed in buried concrete pipes is significantly affected by the pipe diameter, pipe wall thickness and backfill height.

2- The recommended bedding factors in the BS are conservative, where the ratio of the bedding factors obtained from the finite element modelling to the design standard bedding factor ranged from 1.03 to 3.08 depending on the installation type, pipe diameter and backfill height. This means that the current design practice is not economic. Furthermore, the BS neglects the effect of the pipe diameter, pipe wall thickness and backfill height, which have been shown to have significant impact on the bedding factor.

3- Regarding the bedding factors recommended by AASHTO, the ratio of the bedding factor calculated from the finite element modelling to the design standard bedding factor ranged from 0.61 to 2.08. Furthermore, the AASHTO design standard neglects the effect of the pipe wall thickness and backfill height, which have been shown to significantly affect the bedding factor. Therefore, it is suggested that the AASHTO recommended bedding factors could be improved considering these other factors as suggested in this paper.

4- New soil load bedding factor models were developed in this study using an advanced technique based on artificial intelligence called the evolutionary polynomial regression. The models were developed using the bedding factors obtained from the results of the finite element modelling. These models account for the effect of the pipe diameter, pipe wall thickness and backfill height. Hence, a more economic and robust design can be achieved by using the models from this study.

5- Excellent agreement was obtained when the results of the soil load bedding factor model for a Type 2 installation was compared with the bedding factor obtained from a real pipe test by MacDougall et al., (2016), providing confidence in the methodology adopted in this paper.

Acknowledgment

The first author thanks the financial support for his PhD study provided by the higher committee for education development in Iraq (HCED).

References

AASHTO. AASHTO LRFD Bridge Design Specifications. 6th ed. 2013 interim revisions. Washington (DC): AASHTO; 2013.

AASHTO. AASHTO LRFD Bridge Design Specifications. 6th ed. Washington (DC): AASHTO; 2012.

AASHTO. AASHTO LRFD Bridge Design Specifications. 7th ed. 2016 interim revisions. Washington (DC): AASHTO; 2016.

ACI. Building code requirements for structural concrete (ACI 318-14) and commentary (ACI 318R-14). Farmington Hills, MI: American Concrete Institute; 2014.

Ahangar Asr A, Javadi A. Air losses in compressed air tunnelling: a prediction model. Proceedings of the Institution of Civil Engineers-Engineering and Computational Mechanics 2016; 169(3): 140-147.

Alani AM, Faramarzi A, Mahmoodian M, Tee KF. Prediction of sulphide build-up in filled sewer pipes. Environmental Technology 2014; 35(14): 1721-1728.

Allard E, El Naggar H. Pressure distribution around rigid culverts considering soil-structure interaction effects. International Journal of Geomechanics 2016; 16(2): 04015056.

Alzabeebee S, Chapman D, Jefferson I, Faramarzi A. The response of buried pipes to UK standard traffic loading. Proceedings of the Institution of Civil Engineers-Geotechnical Engineering 2017; 170(1), 38-50.

Alzabeebee S, Chapman DN, Jefferson I, Faramarzi A. 2016. Investigating the maximum soil pressure on a concrete pipe with poor haunch support subjected to traffic live load using numerical modelling. In: 11th Pipeline Technology Conference Berlin, Germany; 2016.

Balkaya M, Moore I, Sağlamer A. Study of nonuniform bedding support because of erosion under cast iron water distribution pipes. Journal of Geotechnical and Geoenvironmental Engineering 2012a; 138 (10): 1247–1256.

Balkaya M, Moore ID, Sağlamer A. Study of non-uniform bedding due to voids under jointed PVC water distribution pipes. Geotextiles and Geomembranes 2012b; 34: 39–50.

Balkaya M, Moore ID, Sağlamer A. Study of non-uniform bedding support under continuous PVC water distribution pipes. Tunnelling and Underground Space Technology 2013; 35: 99–108.

Boscardin MD, Selig ET, Lin RS, Yang GR. Hyperbolic parameter for compacted soils. Journal of Geotechnical Engineering ASCE 1990; 116 (1): 88–104.

Brown SF, Selig ET. The design of pavement and rail track foundations. In: O'Reilly MP, Brown SF, editors. Cyclic loading of soils: from theory to practice. Glasgow and London: Blackie and Son Ltd; 1991, p. 249-305.

BSI. BS 9295. Guide to the structural design of buried pipelines. London: BSI; 2010.

Dhar AS, Moore ID, McGrath TJ. Two-dimensional analyses of thermoplastic culvert displacements and strains. Journal of Geotechnical and Geoenvironmental Engineering 2014; 130 (2): 199–208.

Duncan JM, Chang C. Nonlinear analysis of stress and strain in soils. Journal of the Soil Mechanics and Foundations Division ASCE 1970; 96 (5): 1629–1653.

Faramarzi A, Alani AM, Javadi AA. An EPR-based self-learning approach to material modelling. Computers and Structures 2014; 137: 63-71.

Faramarzi A, Javadi AA, Ahangar-Asr A. Numerical implementation of EPR-based material models in finite element analysis. Computers and Structures 2013; 118: 100-108.

Faramarzi A, Javadi AA, Alani AM. EPR-based material modelling of soils considering volume changes. Computers and Geosciences 2012; 48: 73-85.

Giustolisi O, Savic DA. A symbolic data-driven technique based on evolutionary polynomial regression. Journal of Hydroinformatics 2006; 8(3): 207-222.

Giustolisi O, Savic DA. Advances in data-driven analyses and modelling using EPR-MOGA. Journal of Hydroinformatics 2009; 11(3-4): 225-236.

Javadi AA, Faramarzi A, Ahangar-Asr A. Analysis of behaviour of soils under cyclic loading using EPR-based finite element method. Finite Elements in Analysis and Design 2012; 58: 53-65.

Kang J, Jung Y, Ahn Y. Cover requirements of thermoplastic pipes used under highways. Composites Part B-Engineering 2013a; 55: 184-192.

Kang J, Parker F, Yoo CH. Soil-structure interaction and imperfect trench installation for deeply buried concrete pipes. Journal of Geotechnical and Geoenvironmental Engineering 2007; 133 (3): 277-285.

Kang J, Parker F, Yoo CH. Soil–structure interaction for deeply buried corrugated steel pipes Part I: Embankment installation. Engineering Structures 2008a, 30(2): 384-392.

Kang J, Parker F, Yoo CH. Soil–structure interaction for deeply buried corrugated steel pipes Part II: Imperfect trench installation. Engineering Structures 2008b; 30(3): 588-594.

Kang J, Stuart SJ, Davidson JS. Analytical study of minimum cover required for thermoplastic pipes used in highway construction. Structure and Infrastructure Engineering 2014; 10(3): 316-327.

Kang JS, Stuart SJ, Davidson JS. Analytical evaluation of maximum cover limits for thermoplastic pipes used in highway construction. Structure and Infrastructure Engineering 2013b; 9(7): 667-674.

Katona MG. Influence of soil models on structural performance of buried culverts. International Journal of Geomechanics 2017; 17 (1), 04016031.

Kim K, Yoo CH. Design loading on deeply buried box culverts. Journal of Geotechnical and Geoenvironmental Engineering 2005; 131(1): 20-27.

MacDougall K, Hoult NA, Moore ID. Measured load capacity of buried reinforced concrete pipes. ACI Structural Journal 2016; 113 (1): 63-73.

MacDougall K. Behaviour and design of reinforced concrete pipes. MASc thesis. Canada: Queens University; 2014.

Mai VT, Moore ID, Hoult NA. Performance of two-dimensional analysis: Deteriorated metal culverts under surface live load. Tunnelling and Underground Space Technology 2014; 42: 152-160.

Meguid MA, Kamel S. A three-dimensional analysis of the effects of erosion voids on rigid pipes. Tunnelling and Underground Space Technology 2014; 43: 276-289.

Moore ID. Buried pipes and culverts. In: Rowe RK, editor. Geotechnical and Geoenvironmental Engineering Handbook. Norwell: Kluwer Academic Publishing: 2001, p. 539‑566.

Moore ID, Hoult NA, MacDougall K. Establishment of Appropriate Guidelines for Use of the Direct and Indirect Design Methods for Reinforced Concrete Pipe, Contractor's Final Report for NCHRP Project 20-07 Task 316, March 2014 National Cooperative Highway Research Program, National Academy of Sciences Transportation Research Board, Washington D.C.126 pp; 2014.

Moser AP, Folkman S. Buried pipe design, 3rd ed. Stamford: The McGraw-Hill; 2008.

Petersen DL, Nelson CR, Li G, McGrath TJ, Kitane Y. NCHRP Report 647: Recommended design specifications for live load distribution to buried structures, Washington: Transportation Research Board; 2010.

Pettibone HC, Howard AK. Distribution of soil pressures on concrete pipe. Journal of the pipeline division 1967; 93(2): 85-102.

Savic D, Giustolisi O, Berardi L, Shepherd W, Djordjevic S, Saul A. Modelling sewer failure by evolutionary computing. Proceedings of the Institution of Civil Engineers - Water Management 2006; 159(2): 111-118.

Tan Z, Moore ID. Effect of backfill erosion on moments in buried rigid pipes. In: Transportation Research Board Annual Conference, Transportation Research Board, Washington DC, USA; 2007.

Wong LS, Allouche EN, Dhar AS, Baumert M, Moore ID. Long-term monitoring of SIDD type IV installations. Canadian Geotechnical Journal 2006; 43(4): 392-408.

Xu M, Shen D, Rakitin B. The longitudinal response of buried large-diameter reinforced concrete pipeline with gasketed bell-and-spigot joints subjected to traffic loading. Tunnelling and Underground Space Technology 2017; 64: 117-132.

Young OC, O'Reilly MP. A guide to design loadings for buried rigid pipes, Second Impression, London: Department of Transport; 1987.